# Gas Permeation Properties in a Composite Mesoporous Alumina Ceramic Membrane

**Hong-Joo Lee**[*,†], **Hiroyuki Suda and Kenji Haraya**

Research Institute for Innovation in Sustainable Chemistry,
National Institute of Advanced Industrial Science and Technology (AIST), 1-1-1 Higashi, Tsukuba, Ibaraki 305-8565, Japan
(*Received 21 February 2005 • accepted 9 May 2005*)

**Abstract**−In this study, the effect of different chemical interactions on the gas permeation properties were investigated in the composite mesoporous ceramic membrane prepared with $\gamma$-alumina on the surface of a macroporous ceramic membrane. In the permeation results, the gas permeance of the strongly adsorbing gas species increased in the mesoporous ceramic membranes. It is considered that the permeation of the adsorbing gas species increased through preferential adsorption on the membrane pore surface. It was shown in this study that the modified mesoporous ceramic membrane could increase the permeation performance in the presence of the adsorbing gas species due to the surface diffusion mechanism.

Key words: Alumina Ceramic Membrane, Gas Permeance, Mesoporous Membrane, Surface Diffusion

## INTRODUCTION

The first widespread use of polymeric membranes for separation applications dates back to the 1960-70s when cellulose acetate was cast for desalination of sea and brackish waters. Since then many new polymeric membranes have come to the market for applications including ultrafiltration, microfiltration, electrodialysis, and gas separation [Burggraaf and Cot, 1996]. Since the 1980s the industrial application of gas separation has grown to become a $150 million/year business. Currently, several polymer materials including polysulfone, polyimide, and cellulose acetate consist of at least 90% of the total installed gas separation membrane processes [Hsieh, 1996].

It was reported that the permeation performance decreased even in the presence of trace quantities of condensable hydrocarbons in the gas separation process using some polymeric membranes. Moreover, plasticization of the selective skin layer by extremely high partial pressures of $CO_2$ is also known to occur in the polymeric membrane processes [Rautenbach and Welsh, 1994; White et al., 1995; Bhide and Stern, 1993]. Interest in inorganic membrane processes including zeolite, carbon and ceramic membranes has increased in many application areas since they have high gas permeances and represent thermal, chemical and mechanical stabilities compared with glassy polymeric membranes [Jung et al., 1999; Koros and Mahajan, 2000; Koros and Flemming, 1993; Lin, 2001; Hasegawa et al., 2002].

In general, gas transport occurring in polymeric membranes is described by the solution-diffusion mechanism, which consists of the following consecutive steps: sorption in membrane structure, diffusion through membrane and desorption on the other side of membrane. Unlike the gas transport mechanism for polymeric membranes, gas transport through inorganic membranes is more complex. It is accepted that the mechanisms for gas transport through

inorganic membranes are primarily varied with pore size distribution and to some extent with chemical interaction between the diffusing gas species and the membrane materials [Gallaher and Liu, 1994; Moon et al., 2004]. Basically, gas transported through inorganic membranes is classified with four mechanisms: Knudsen diffusion, molecular sieving, capillary condensation, and surface diffusion.

A gas molecule diffuses into the membrane pores and then progresses only by collisions with the pore wall in the Knudsen diffusion mechanism, showing a high gas permeance but a low selectivity. In addition, gas separation occurs by molecular sieving when the pore dimensions of the inorganic membranes approach those of the diffusing gas species. Nearly infinite separation factors are theoretically attainable in this mechanism, even though the permeances are low [Geiszler and Koros, 1996; Suda and Haraya, 2000; Wang et al., 2003]. Meanwhile, capillary condensation can occur in the pores of the membranes having a mesoporous structure in the presence of condensable gas species such as water vapor and butane. The high permeance and high selectivity in this mechanism are observed due to the pore filling of condensable gas species in the membrane structure [Lee and Hwang, 1986; Uhlhorn et al., 1992; Yoshioka et al., 2004]. When the adsorption of adsorbing gas species occurs on the surface of the membrane pores the performance of gas transport increases by so-called surface diffusion mechanism [Moon et al., 2004; Cooper and Lin, 2002]. The gas species with a high adsorption capacity is preferentially adsorbed on the pores of the membrane, reducing open porosity and then limiting the diffusion of the weakly adsorbing gases into the pores. Therefore, the adsorbing gas species show higher permeance in porous materials than predicted from the Knudsen diffusion [Uchytil et al., 2003; Rao and Sircar, 1996; Fuertes, 2000].

Of inorganic membranes, ceramic membranes with a wide range of pore sizes can be prepared by using various methods for many different applications [Kim et al., 2001; Jung et al., 1999]. The composite ceramic membranes having a mesoporous $\gamma$-alumina layer on a macroporous $\alpha$-alumina are considered as one of the effective preparation methods to reduce the pore size or to improve the specific surface properties for high gas permeances [Pan et al., 1999; Kim

**Table 1. Characteristic properties of ceramic membranes**

| | Support | Active layers | |
|---|---|---|---|
| | | $\alpha$-alumina | $\gamma$-alumina |
| Average pore size* | 0.7 μm | 0.06 μm | 4 nm |
| Porosity | 39% | 40% | 40% |
| Calcination temperature | - | 900-1,000 °C | 600 °C |

*The pore size distributions were measured by using the mercury intrusion method.

and Sea, 2001]. In this study, the gas permeation properties having different adsorbing capacity were investigated for the $\gamma$-alumina ceramic membrane prepared on the surface of the macroporous ceramic support. Also, the influence of adsorption on the gas transport and permeation performance was investigated in the mesoporous $\gamma$-alumina ceramic membrane.

## EXPERIMENTAL

In this study, the ceramic alumina support is an asymmetric and composite ceramic membrane (Noritake, Japan) having an average pore diameter of 0.7 μm and a porosity of 39%. The $\alpha$-alumina ceramic membrane was prepared on the surface of the alumina support. And the composite $\gamma$-alumina ceramic membrane was prepared on the surface of the $\alpha$-alumina ceramic membrane. Table 1 shows the characteristic properties of the ceramic membranes including the alumina support, $\alpha$-alumina and $\gamma$-alumina membranes. The cross-section of the composite $\gamma$-alumina ceramic membranes and the thickness of two alumina ($\alpha$-alumina and $\gamma$-alumina) layers were observed by using a scanning electron microscope (SEM) (S-900, Hitachi). The surface adsorption property of the $\gamma$-alumina layer was characterized by the nitrogen adsorption/desorption at 77 K with an automatic adsorption apparatus, BELSORP-18 (BEL-Japan Inc., Japan), after $\gamma$-alumina particles were pretreated at 300 °C during 5 hours in a vacuum condition. In addition, different adsorption capacity of some gas species was compared by the measurement of the adsorbed amount on the surface of the $\gamma$-alumina layer at 25 °C.

In this study, gas species having different adsorption capacity were selected, such as the weakly adsorbing species (He, $N_2$, and $CH_4$) and the strongly adsorbing species ($CO_2$ and $C_2H_6$). The permeance of gas species was measured by using a permeation apparatus having a film flow meter at a pressure range lower than 180 KPa and a temperature range between 25 °C (298 K) and 150 °C (423 K). The permeation performance of $\alpha$-alumina and $\gamma$-alumina ceramic membranes was compared through permeation experiments. And the gas transport mechanisms were considered for the permeation properties in this study.

In the gas transport and separation for the binary mixture gas system in the presence of the adsorbing species, the gas compositions of permeate were analyzed with a gas chromatograph, Ohkura 802, Japan with a thermal conductivity detector (TCD). Helium was used as a carrier gas through 200 cm-long Porapak Q packed column (50/80 mesh). The permselectivity in the single gas system was estimated as the permeance ratio of each gas species in the permeate side. For the binary mixture gas system, the selectivity was defined as the ratio of the gas composition in the permeate side to the feed
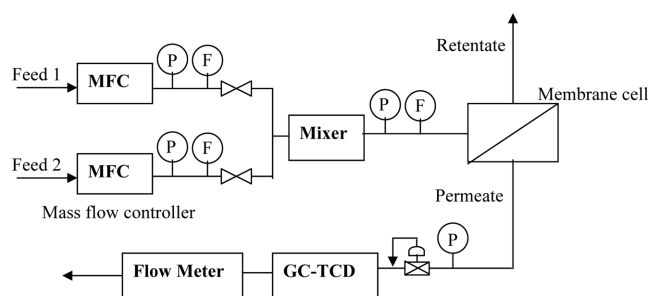
**Fig. 1. Schematic diagram of the permeation experiments.**

one. In addition, long term experiments were carried out for the $\gamma$-alumina ceramic membrane stored at a room condition. A schematic diagram of the permeation measurement for the single and binary mixture gas systems is shown in Fig. 1.

## RESULTS AND DISCUSSION

### 1. Morphology of Membranes and Adsorption Properties of $\gamma$-Alumina Layer

The cross section of the $\gamma$-alumina ceramic membrane was observed by using a SEM, and the analyzed result shows that the membrane consists of the support layer and the two active layers ($\alpha$-alumina and $\gamma$-alumina). The thickness of the $\alpha$-alumina and the $\gamma$-alumina layers was estimated as 81±2 μm and 4.1±0.2 μm, respectively (See Fig. 2). When a gas species comes into contact with a pore surface, gas molecules adsorb to the surface in quantities depending on their partial pressure. The measurement of the adsorbed amount over a range of partial pressure at a single temperature results in an adsorption isotherm. It is generally accepted that the adsorption isotherm shows different types depending on the pore structure of a porous media and intermolecular interactions between the gas and the surface. Fig. 3(a) shows the nitrogen adsorption/desorption isotherm, similar with the Type IV physisorption isotherm according to the BDDT (Brunauer, Deming, Deming, and Teller)
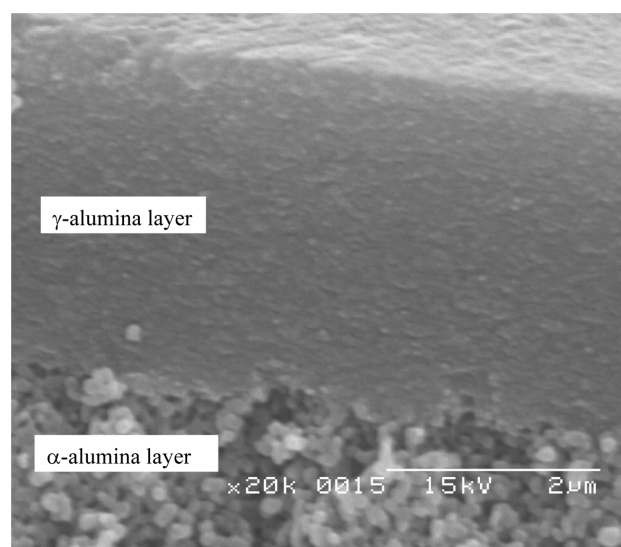


**Fig. 2. Cross-section image for the $\gamma$-alumina ceramic membrane having two active layers.**
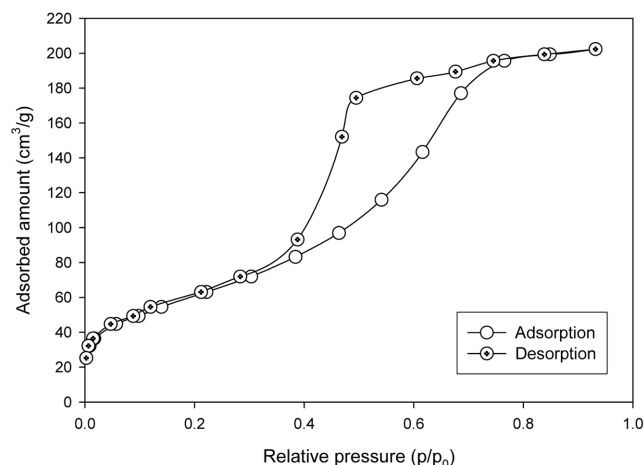
(a) Adsorption-desorption isotherm
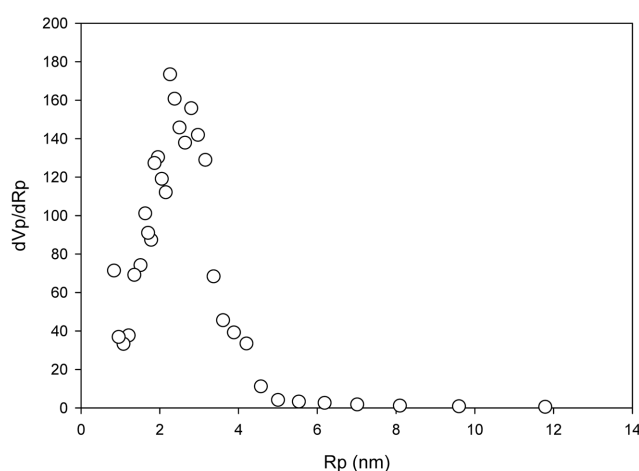


(b) Pore size distribution

**Fig. 3. Characterization of pore properties of γ-alumina layer by the nitrogen adsorption.**

classification [Sing et al., 1985]. The monolayer and multilayer adsorption can be observed in the Type IV isotherm, occurring in the mesoporous structures between 2 and 50 nm [Nagamine et al., 2001; Choi et al., 2001].

Determination of the pore size in the membrane structure and its distribution is of importance for preparation, characterization, and application for gas separation since their properties are related to the gas permeation performance. Based on the nitrogen adsorption measurement results, the pore size distribution for the γ-alumina layer was estimated by the Barrett, Joyner, and Halenda (BJH) method. Fig. 3(b) shows that it has a mesoporous structure with the peak radius of 2.26 nm (mean pore diameter 4.5 nm). The pore size has a somewhat narrow distribution and most of the pores exist below a radius of 5 nm. The estimated result of the average pore size of the γ-alumina layer was similar with the reported one from the company by using the mercury intrusion method, as shown in Table 1.

**2. Permeation Performances in the Alumina Ceramic Membranes**

The results for the gas permeation experiments with the α-alumina and γ-alumina ceramic membranes are summarized in Table 2 in terms of the gas permeance and the permselectivity. It is shown

**Table 2. Modification of the permeation performance in the γ-alumina membrane**

(a) Gas permeance

| | Molecular weight | Permeance (mol/m²secPa) | |
|---|---|---|---|
| | | α-alumina membrane | γ-alumina membrane |
| He | 4 | 13.39 | 5.72 |
| $CH_4$ | 16 | 8.66 | 2.22 |
| $N_2$ | 28 | 6.55 | 1.59 |
| $C_2H_6$ | 30 | 6.75 | 2.11 |
| $CO_2$ | 44 | 5.60 | 1.51 |

(b) Permselectivity with $CO_2$

| | α-alumina membrane | γ-alumina membrane | Ideal selectivity* |
|---|---|---|---|
| $He/CO_2$ | 2.39 | 3.80 | 3.32 |
| $CH_4/CO_2$ | 1.55 | 1.47 | 1.66 |
| $N_2/CO_2$ | 1.17 | 1.05 | 1.25 |
| $C_2H_6/CO_2$ | 1.20 | 1.40 | 1.20 |

*The ideal selectivity was estimated by Knudsen diffusion.

in the table that the permeances of gas species in the modified membrane with γ-alumina layer decreased to one-third or one-fourth compared with results of the α-alumina membrane. The permeation result of He in the γ-alumina membrane showed the smallest decrease due to a small molecular weight (See Table 2(a)). Considering the permeation results for α-alumina and γ-alumina membranes, He and $CH_4$ showed high permeances, while the permeance of $CO_2$ was measured to the lowest value. The result implies that the gas transport through both membranes was mainly affected by the Knudsen diffusion mechanism. In the case of $C_2H_6$, however, the permeance showed $2.1 \times 10^{-6}$ mol/m²secPa, a much higher value compared with that of $N_2$ ($1.6 \times 10^{-6}$ mol/m²secPa) in the mesoporous γ-alumina ceramic membrane. The result implies that the gas permeation increased in the both alumina membranes by an additional mechanism as well as by the Knudsen diffusion [Uchytil et al., 2003; Yoshioka et al., 2004].

The permselectivities with $CO_2$ in Table 2(b) showed similar values with the ideal selectivity estimated by the Knudsen diffusion. However, it is noted that the selectivity of $C_2H_6/CO_2$ was higher than expected by the Knudsen diffusion. The value of the selectivity of $C_2H_6/CO_2$ is 1.40 for the γ-alumina membrane, which is higher than that of $N_2/CO_2$ (1.05). The higher permeation performance of $C_2H_6$ through the mesoporous ceramic membrane is related to adsorption capacity, which is determined by the adsorption isotherm. Of gas species, the adsorption amount of the adsorbing gas species ($CO_2$ and $C_2H_6$) on the surface of γ-alumina layer was measured and the results are shown in Fig. 4. In the figure the adsorption capacity of $C_2H_6$ is much higher than that of $CO_2$, about two times when the pressure approaches 1 atm (101.3 KPa). It is considered that the permeance of the strongly adsorbing gas species ($C_2H_6$) in the γ-alumina ceramic membrane increased through preferential adsorption on the pore surface due to the surface diffusion mechanism [Moon et al., 2004; Fuertes, 2000].

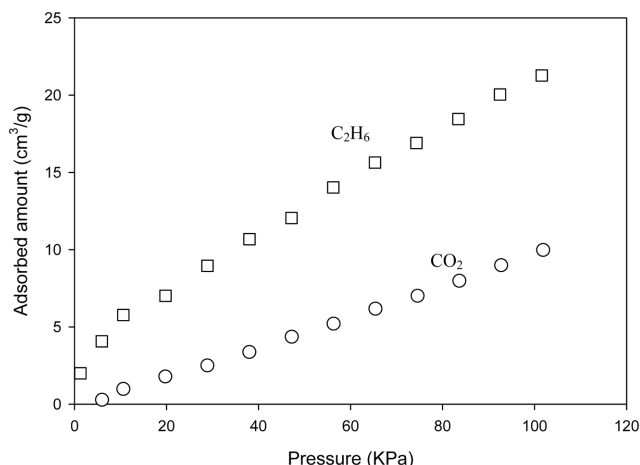In addition, chemical interaction of the diffusion gas molecules

Fig. 4. Adsorption capacities of $CO_2$ and $C_2H_6$ on the surface of $\gamma$-alumina layer.

**Table 3. Estimated resistances of alumina ceramic membranes**

| | Resistance $(10^{-6}$ mol/secPa$)^{-1}$ | | Resistance ratio* |
|---|---|---|---|
| | Total resistance | $\gamma$-alumina layer resistance | |
| He | 515 | 330 | 0.64 |
| $CH_4$ | 1330 | 510 | 0.62 |
| $N_2$ | 1854 | 675 | 0.64 |
| $C_2H_6$ | 1400 | 655 | 0.53 |
| $CO_2$ | 1956 | 789 | 0.60 |

*The value represents the ratio of the $\gamma$-alumina layer resistance to the total resistance.

can give an effect on the resistance for the gas transport through the membrane pores. The gas transport resistance for the $\gamma$-alumina layer was estimated so as to investigate the adsorption influence on the resistance through the alumina ceramic membranes [Hamad et al., 2001]. The total resistance in the $\gamma$-alumina ceramic membrane consisting of the support and the two active layers, $R_t$, can be estimated by the following equation:

$$R_t = \frac{1}{A(P/\delta)}. \tag{1}$$

Here, A is the effective membrane area for the gas permeation and $(P/\delta)$ the gas permeance. The above equation implies that gas species with a higher molecular weight represents a higher total resistance due to its lower permeance. Table 3 shows an estimated total resistance for each gas species using Eq. (1). As predicted by the Knudsen diffusion mechanism, He showed the least resistance and $CO_2$ the highest among examined gas species. It is noted that the total resistance of $C_2H_6$ showed much lower value than $N_2$, suggesting that the adsorption on the surface of the pore structure reduced the resistance of the gas transport through membranes.

Like the results in the total resistance, the transport resistance of $C_2H_6$ in the $\gamma$-alumina layer was somewhat lower than that of $N_2$. Considering the ratio of $\gamma$-alumina layer resistance to total resistance, the estimated values were dependent on the adsorbing capacity, as discussed before. The values of the weakly adsorbing gas species (He, $CH_4$, and $N_2$) represented 0.6 or higher. Meanwhile,
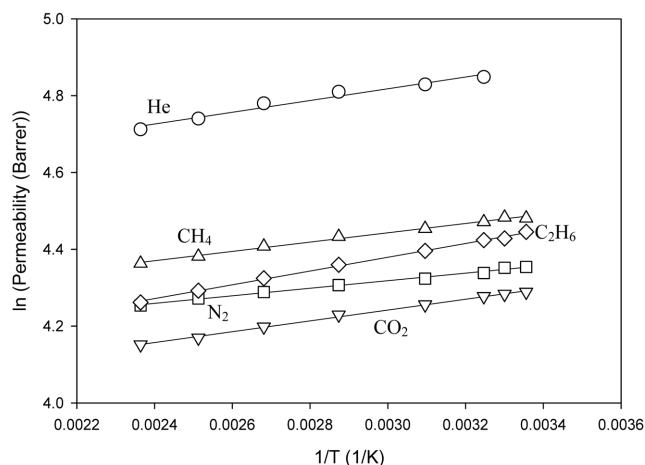
Fig. 5. Relationship between permeation temperature and permeability in the $\gamma$-alumina membrane.

the strongly adsorbing gas species ($C_2H_6$) showed the lowest value. The investigation of the adsorption influence on the gas transport resistance showed that the resistance of gas transport through membranes was decreased by the adsorption on the surface of the pore structure.

The value of activation energy is an indicator of the barrier for gas transport in gas separation membranes. That is, a lower value of the activation energy represents a lower resistance for gas transport through membranes. Fig. 5 shows the relationship between permeation temperature and its corresponding permeability for the $\gamma$-alumina mesoporous ceramic membrane. The estimated results for the activation energy show that $C_2H_6$ represented the lowest value, $-1.49$ KJ/mol. In the case of $CO_2$ having lower adsorption capacity than $C_2H_6$ shown in Fig. 4, the activation energy was estimated as $-1.17$ KJ/mol. Moreover, the weakly adsorbing gas species showed less negative values, that is, $-1.01$ KJ/mol for $N_2$ and $-0.82$ KJ/mol for $CH_4$, respectively. The result implies that the adsorption on the pore surface decreased resistance for gas transport, thus increasing gas permeance performance especially for the adsorbing gas species through mesoporous ceramic membranes [Kim et al., 2001].

## 3. Consideration of Transport Mechanisms through the Mesoporous Membrane

A characteristic feature of gas transport by the Knudsen diffusion mechanism is that the permeance shows an inverse square root dependence on temperature and molecular weight of the diffusing gas molecules, assuming that there is no involvement of chemical interaction. The expression for the Knudsen flow in a porous medium can be written by using the Knudsen equation, as follows:

$$P_k = \frac{J_k}{\Delta P/\delta} = \frac{2}{3}\frac{\varepsilon r}{\tau}\sqrt{\frac{8}{\pi RTM}} \tag{2}$$

where $P_k$ is the permeability due to the Knudsen diffusion mechanism, $J_k$ the Knudsen flux, $\varepsilon$ the porosity, $\tau$ the tortuosity factor, r the pore radius and M molecular weight of gas species. Fig. 6 shows the relationship between the permeance and the molecular weights of gas species. The measured permeances of the weakly adsorbing gas species (He, $CH_4$, and $N_2$) are inversely proportional to square root of molecular weight as expressed in Eq. (2). However, the ad-
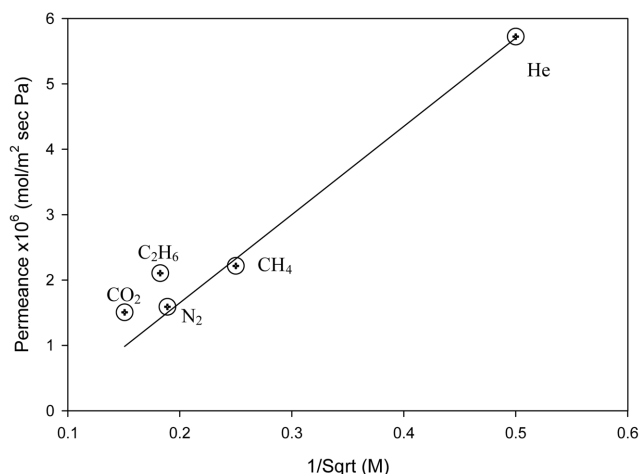
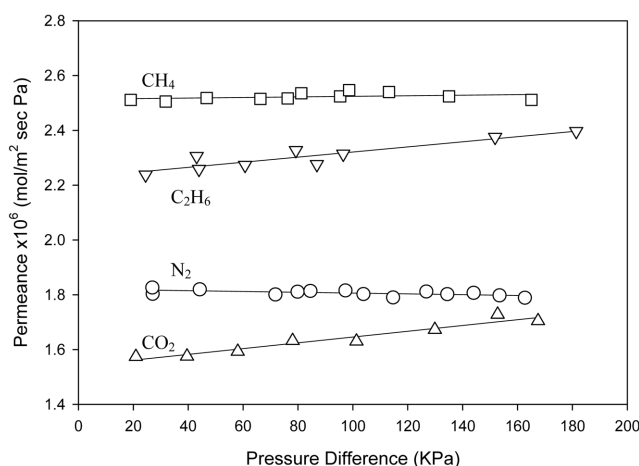Fig. 6. Relationship between permeance and molecular weight in the γ-alumina membrane.



Fig. 7. Effect of the pressure on gas permeance in the γ-alumina membrane.



Fig. 8. Relationship between $P_k(MT)^{1/2}$ and permeation temperature in the γ-alumina membrane.

sorbing gas species ($CO_2$ and $C_2H_6$) showed a deviation from the linear relationship, implying that the permeance increased due to an additional transport mechanism, the surface diffusion, as discussed before.

Considering the relationship between the permeation pressure and the permeance in Eq. (2), the permeability or permeance due to the Knudsen diffusion is independent of the permeation pressure. Fig. 7 shows the permeation plots for the weakly adsorbing gases ($CH_4$ and $N_2$) and strongly adsorbing gases ($CO_2$ and $C_2H_6$) in the relationship between the permeation pressure and the permeance. It can be observed that the permeance of the $CH_4$ and $N_2$ is independent of the pressure in the membrane, which is in complete agreement with the expected Knudsen flux in the pores [Uchytil et al., 2003]. In the case of adsorbing gases ($CO_2$ and $C_2H_6$), their permeances increased with increasing pressure in the membrane. The permeance of $CO_2$ increased from $1.6 \times 10^{-6}$ mol/m²secPa at 20 KPa to $1.7 \times 10^{-6}$ mol/m²secPa at 170 KPa. In addition, that of $C_2H_6$ increased from 2.2 to $2.4 \times 10^{-6}$ mol/m²secPa with increasing pressures. The results imply that the surface diffusion mechanism contributes to the permeance of adsorbing gases ($CO_2$ and $C_2H_6$)
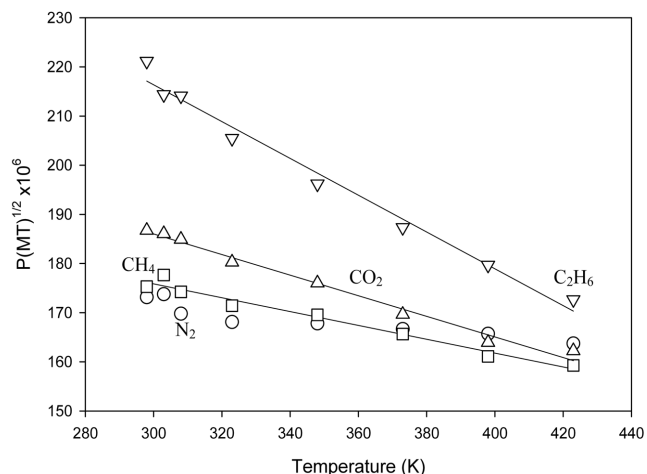
through the pores in the mesoporous membranes [Lee and Oyama, 2002].

The above Eq. (2) can be rewritten as follows:

$$P_k(MT)^{1/2} = \left(\frac{\varepsilon d}{\tau \delta}\right)\left(\frac{8}{9\pi R}\right)^{1/2}. \qquad (3)$$

Here, $\varepsilon$, $\tau$, d and $\delta$ are parameters related to the properties of a membrane rather than those of permeating gas species. Therefore, every permeating gas molecule should have the same slope in the relationship between $P_k(MT)^{1/2}$ and temperature, independent of temperature if gas transport through the membrane is affected only by the Knudsen diffusion [Lee and Oyama, 2002; Kim and Sea, 2001]. Gas permeation data on the γ-alumina ceramic membrane were analyzed in the relationship between $P_k(MT)^{1/2}$ and the permeation temperature (See Fig. 8). Relatively constant values of the slope in the plot were observed for the weakly adsorbing gas species ($N_2$ and $CH_4$) over the applied temperature range (between 25 and 150 °C). It is indicated that the transport of these gases is mainly controlled by the Knudsen diffusion. Meanwhile, the strongly adsorbing gas species ($CO_2$ and $C_2H_6$) showed higher slopes than those for the weakly adsorbing gas species due to the surface diffusion [Fuertes and Menendez, 2002; Fuertes, 2000]. Through analysis of permeation results through the mesoporous γ-alumina ceramic membrane, it is considered that the permeance of the strongly adsorbing gas species, $CO_2$ and $C_2H_6$, increased due to the surface diffusion through the preferential adsorption on the pore surface.

## 4. Permeation Performances in the Binary Mixture Gas System

For permeation performance in the mixture system, the permeation result was considered in the binary mixture system of $C_2H_6$ and $N_2$. Fig. 9 shows the permeation performance (the permeance and the selectivity) in the binary mixture system of $C_2H_6/N_2$ (53 : 47) with increasing permeation temperature. As the permeation temperature increased, the permeance of $N_2$ in the binary mixture system decreased from $1.39 \times 10^{-7}$ to $7.63 \times 10^{-8}$ mol/m²secPa, similar aspect with the results for the single gas systems (See Fig. 9(a)). In the case of the permeation results of $C_2H_6$ in the binary mixture system, the permeance increased with increasing temperature (from $6.31 \times 10^{-7}$
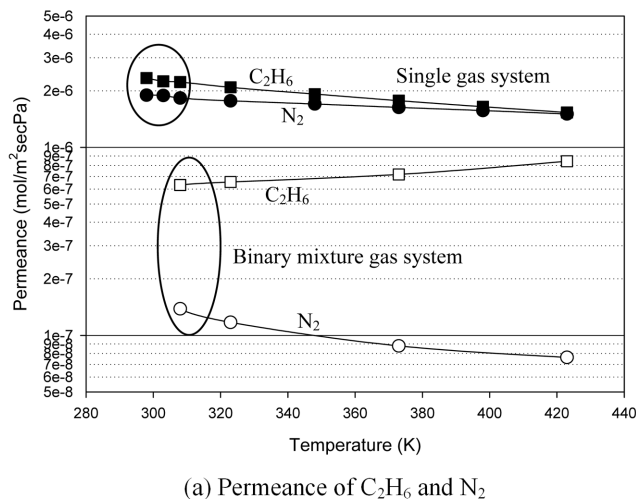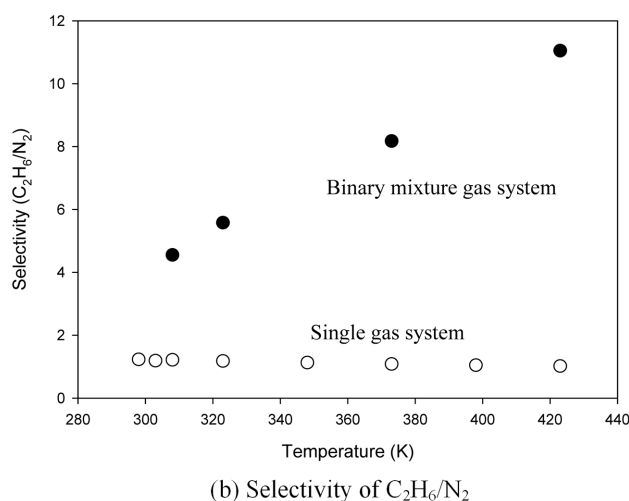
(a) Permeance of $C_2H_6$ and $N_2$



(b) Selectivity of $C_2H_6/N_2$

**Fig. 9. Permeation performance in the binary mixture system of $C_2H_6$ and $N_2$.**



(a) Permeance of $C_2H_6$ and $N_2$



(b) Selectivity of $C_2H_6$ and $N_2$

**Fig. 10. Effect of composition on permeation in the binary mixture system of $C_2H_6$ and $N_2$.**

to $8.43 \times 10^{-7}$ mol/m²secPa). Different from the result in the single gas system, the value of $C_2H_6$ permeance increased with increasing permeation temperature, which can be explained by the surface diffusion mechanism as discussed before. It is considered that the preferential adsorption of $C_2H_6$ decreased the $N_2$ permeance through the mesopores and that the inhibition effect on the $N_2$ permeation increased due to increasing permeance of $C_2H_6$ [Choi et al., 2001; Yoshioka et al., 2004]. Fig. 9(b) shows the selectivity of $C_2H_6/N_2$ in the single and the binary mixture systems with increasing permeation temperature. The effect of the preferential adsorption on the selectivity could be clearly observed in the figure. With increasing temperature, the values of the selectivity in the single gas system were between 1.0 and 1.2. Meanwhile, the selectivity of $C_2H_6/N_2$ increased from 4.6 to 11.0 in the binary mixture system.

Composition of gas species in a mixture gas system also affects the permeation performance (permeance and selectivity). Fig. 10 shows the influence of $C_2H_6$ mole fraction on the permeation results in the binary mixture of $C_2H_6$ and $N_2$ at the permeation temperature of 35 °C. The permeance of $C_2H_6$ was negligibly low at low compositions up to 0.3, and then increased drastically between 0.3 and 0.4. Above 0.4 of the $C_2H_6$ mole fraction, the permeance of $C_2H_6$
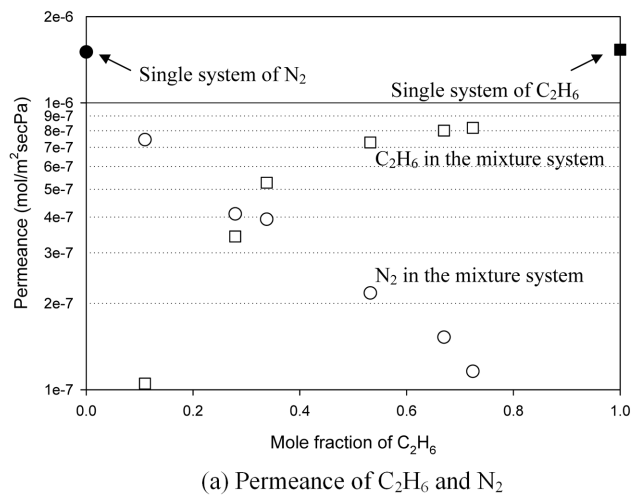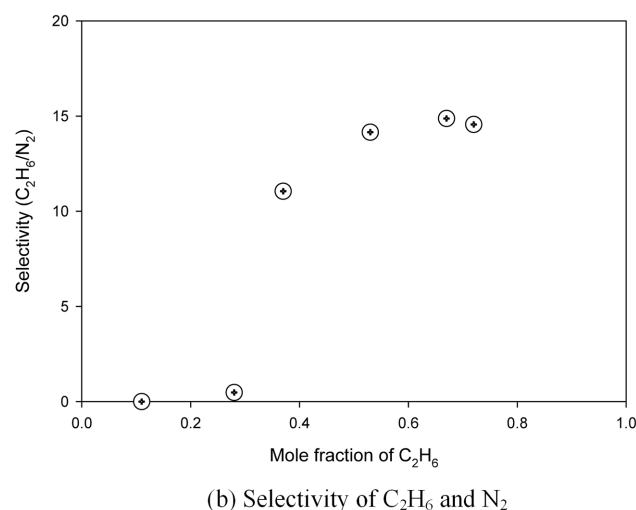
and $N_2$ were not changed (See Fig. 10(a)). Fig. 10(b) shows the selectivity of $C_2H_6/N_2$ with increasing mole fraction of $C_2H_6$. The selectivity of $C_2H_6/N_2$ showed 10-14 above a mole fraction of 0.4. It is considered that a monolayer and then a multilayer adsorption occurred on the pore after the preferential adsorption in the binary system of $C_2H_6$ and $N_2$ as the concentration of $C_2H_6$ increased [Choi et al., 2001; Uchytil et al., 2003].

## 5. Permeation Stability for the Mesoporous Ceramic Membrane

It is accepted that membranes have three key performances affecting their economic utility for large scale applications. The first parameter is their selectivity toward the gases to be separated, affecting directly the recovery of the process and indirectly feed gas flow requirements. The second one is membrane flux or permeance, which simply determines the amount of membrane and capital cost. And the third one is the life of the membrane, which is related to maintenance and replacement costs [Spillman, 1989].

In the previous sections, the influence of the preferential adsorption on the selectivity and the permeance was investigated in the γ-alumina ceramic membrane. The permeation stability during the long term (200 days) for the membrane was considered in this sec-
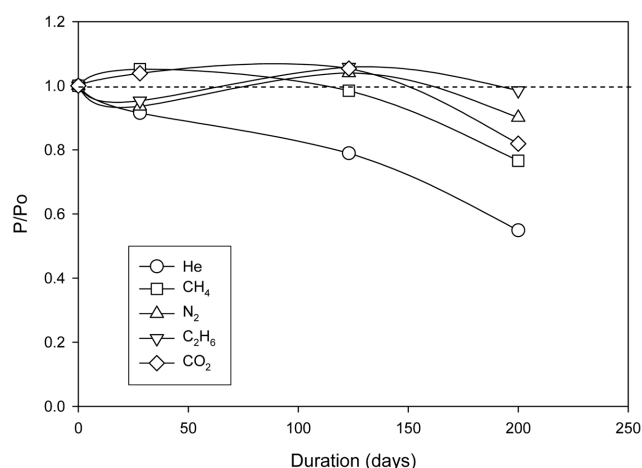
**Fig. 11. Permeance change in the long term permeation experiments.**

**Table 4. Permselectivity changes in the long term permeation experiments**

(a) Permselectivity with $CO_2$

| | Duration | |
|---|---|---|
| | 0 day | 200 days |
| $He/CO_2$ | 3.80 | 2.54 |
| $CH_4/CO_2$ | 1.47 | 1.38 |
| $N_2/CO_2$ | 1.05 | 1.16 |
| $C_2H_6/CO_2$ | 1.40 | 1.68 |

(b) Permselectivity with $CH_4$

| | Duration | |
|---|---|---|
| | 0 day | 200 days |
| $He/CH_4$ | 2.58 | 1.85 |
| $N_2/CH_4$ | 0.72 | 0.84 |
| $C_2H_6/CH_4$ | 0.95 | 1.22 |
| $CO_2/CH_4$ | 0.68 | 0.73 |

tion. Fig. 11 shows the change in the relative permeance ($P/P_0$) for each gas species. In the permeance changes for the weakly adsorbing gas species, He showed the largest decrease as 45% and the permeance of $CH_4$ and $N_2$ was decreased as 23% and 10%, respectively, in the long term permeation experiments. Due to the highest adsorption capacity, a small change in the permeance of $C_2H_6$ was observed with a decrease of only 2%. It is considered in the long term permeation experiments that different permeation results were observed due to different adsorption capacity [Menendez and Fuertes, 2001].

Table 4 summarizes the estimated permselectivities of $CO_2$ and $CH_4$ in the long term permeation experiments. The permselectivities with $CO_2$ ($C_2H_6/CO_2$ and $N_2/CO_2$) showed the increased value due to the smallest decrease in the permeance of $C_2H_6$ and $N_2$ for the long term stability test. Also, the permselectivities with $CH_4$ were increased in the long term permeation experiments due to decrease in the $CH_4$ permeance except for $He/CH_4$. The permselectivity of $C_2H_6/CH_4$ showed the largest increase from 0.95 to 1.22. It is con-

sidered that adsorption of $O_2$ in air increased the adsorption of hydrocarbons on the surface of $\gamma$-alumina membrane, resulting in increasing permeation performance of $C_2H_6$ [Menendez and Fuertes, 2001]. It was observed in the permeation experiment for the stability that $C_2H_6$ showed high permeation performance due to the adsorption capacity.

## CONCLUSIONS

Interest in ceramic membranes has increased in many application areas due to high permeances and their thermal, chemical and mechanical stabilities. In this study, the influence of chemical interaction between the diffusing gas molecules and the membrane pore surface on the gas permeation properties was investigated in the mesoporous $\gamma$-alumina ceramic membrane. In the permeation results the mesoporous ceramic membranes showed high gas permeances, especially for the strongly adsorbing gas species ($CO_2$ and $C_2H_6$) due to the surface diffusion mechanism. In the binary mixture system of $C_2H_6$ and $N_2$, the preferential adsorption of $C_2H_6$ increased its permeance and the selectivity of $C_2H_6/N_2$. Also, the gas species having a high adsorption capacity showed a good performance in the long term stability test. Through the gas transport experiments, it was shown that the preferential adsorption of the adsorbing gas species on the surface of the mesoporous structures could increase gas permeation performance.

## ACKNOWLEDGMENT

## NOMENCLATURE

| | |
|---|---|
| A | : effective membrane area [$m^2$] |
| d | : pore diameter in the membrane [m] |
| $J_k$ | : flux by the Knudsen diffusion [mol/$m^2$sec] |
| M | : molecular weight of gas species |
| P | : permeability [mol m/$m^2$secPa] |
| $P_k$ | : permeability by the Knudsen diffusion [mol m/$m^2$secPa] |
| R | : gas constant [8.314 J/mol K] |
| $R_t$ | : total resistance [mol/secPa]$^{-1}$ |
| T | : temperature [K] |
| r | : pore radius in the membrane [m] |
| $\Delta P$ | : pressure difference [Pa] |
| $\delta$ | : membrane thickness [m] |
| $\varepsilon$ | : porosity |
| $\tau$ | : tortuosity factor |

## REFERENCES

Bhide, B. D. and Stern, S. A., "Membrane Processes for the Removal of Acid Gases from Natural Gas. I. Process Configurations and Optimization of Operating Conditions," *J. Membr. Sci.*, **81**, 209 (1993).

Burggraaf, A. J. and Cot, L., *Fundamentals of Inorganic Membrane Science and Technology*, Elsevier, Amsterdam (1996).

Choi, J. G., Do, D. D. and Do, H. D., "Surface Diffusion of Adsorbed Molecules in Porous Media: Monolayer, Multilayer, and Capillary

Condensation Regimes," *Ind. Eng. Chem. Res.*, **40**, 4005 (2001).

Cooper, C. A. and Lin, Y. S., "Microstructural and Gas Separation Properties of CVD Modified Mesoporous γ-Alumina Membranes," *J. Membr. Sci.*, **195**, 35 (2002).

Fuertes, A. B. and Menendez, I., "Separation of Hydrocarbon Gas Mixtures Using Phenolic Resin-based Carbon Membranes," *Sep. Purif. Tech.*, **28**, 29 (2002).

Fuertes, A. B., "Adsorption-selective Carbon Membrane for Gas Separation," *J. Membr. Sci.*, **177**, 9 (2000).

Gallaher, G. K. and Liu, P. K. T., "Characterization of Ceramic Membranes I. Thermal and Hydrothermal Stabilities of Commercial 40 Å Membranes," *J. Membr. Sci.*, **92**, 29 (1994).

Geiszler, V. C. and Koros, W. J., "Effects of Polyimide Pyrolysis Conditions on Carbon Molecular Sieve Membrane Properties," *Ind. Eng. Chem. Res.*, **35**, 2999 (1996).

Hamad, F. A., Chowdhury, G. and Matsuura, T., "Sulfonated Polyphenylene Oxide-Polyethersulfone Thin-film Composite Membranes: Effect of Counterions on the Gas Transport Properties," *J. Membr. Sci.*, **191**, 71 (2001).

Hasegawa, Y., Tanaka, T. and Watanabe, K., "Separation of $CO_2$-$CH_4$ and $CO_2$-$N_2$ System Using Ion-exchange FAU-Zeolite Membrane with Different Si/Al Ratios," *Korean J. Chem. Eng.*, **19**, 309 (2002).

Hsieh, H. P., *Inorganic Membranes for Separation and Reaction,* Elsevier, Amsterdam (1996).

Jung, K. Y., So, J. H., Park, S. B. and Yang, S. M., "Hydrogen Separation from the $H_2$/$N_2$ Mixture by Using a Single and Multi-stage Inorganic Membrane," *Korean J. Chem. Eng.*, **16**, 193 (1999).

Kim, S. S. and Sea, B. K., "Gas Permeation Characteristics of Silica/alumina Composite Membrane Prepared by Chemical Vapor Deposition," *Korean J. Chem. Eng.*, **18**, 322 (2001).

Kim, Y. S., Kusakabe, K., Morooka, S. and Yang, S. M., "Preparation of Microporous Silica Membranes for Gas Separation," *Korean J. Chem. Eng.*, **18**, 106 (2001).

Koros, W. J. and Flemming, G. K., "Membrane-based Gas Separation-Review," *J. Membr. Sci.*, **83**, 1 (1993).

Koros, W. J. and Mahajan. R., "Pushing the Limits on Possibilities for Large Scale Gas Separation: Which Strategies?" *J. Membr. Sci.*, **175**, 181 (2000).

Lee, D. and Oyama, S. T., "Gas Permeation Characteristics of a Hydrogen Selective Supported Silica Membrane," *J. Membr. Sci.*, **210**, 291 (2002).

Lee, K. H. and Hwang, S. T., "The Transport of Condensable Vapors through a Microporous Vycor Glass Membrane," *J. Colloid Interf. Sci.*, **110**, 544 (1986).

Lin, Y. S., "Microporous and Dense Inorganic Membranes: Current Status and Prospective," *Sep. Purif. Tech.*, **25**, 39 (2001).

Menendez, I. and Fuertes, A. B., "Aging of Carbon Membranes Under Different Environments," *Carbon*, **39**, 733 (2001).

Moon, J. H., Ahn, H., Hyun, S. H. and Lee, C. H., "Separation Characteristics of Tetrapropylammoniumbromide Templating Silica/alumina Composite Membrane in $CO_2$/$N_2$, $CO_2$/$H_2$ and $CH_4$/$H_2$ Systems," *Korean J. Chem. Eng.*, **21**, 477 (2004).

Nagamine, S., Endo, A., Nakaiwa, M., Nakane, T., Kurumada, K. I. and Tanigaki, M., "Synthesis of Submillimeter-thick Films of Surfactant Templated Mesoporous Silica," *Micropor. Mesopor. Mat.*, **43**, 181 (2001).

Pan, M., Cooper, C. A., Lin, Y. S. and Meng, G. Y., "CVD Modification and Vapor/gas Separation Properties of Nanoporous Alumina Membranes," *J. Membr. Sci.*, **158**, 235 (1999).

Rao, M. B. and Sircar, S., "Performance and Pore Characterization of Nanoporous Carbon Membranes for Gas Separation," *J. Membr. Sci.*, **110**, 109 (1996).

Rautenbach, R. and Welsch, K., "Treatment of Landfill Gas by Gas Permeation-Pilot Plant Results and Comparison to Alternatives," *J. Membr. Sci.*, **87**, 107 (1994).

Sing, K. S. W., Everett, D. H., Haul, R. A. W., Mosocou, L., Pirtotti, R. A., Rouqurol, J. and Siemieniewska, T., "Reporting Physisorption Data for Gas/solid Systems," *Pure & Appl. Chem.*, **57**, 603 (1985).

Spillman, R. W., "Economics of Gas Separation Membranes," *Chem. Eng. Prog.*, **85**, 41 (1989).

Suda, H. and Haraya, K., "Carbon Molecular Sieve Membranes: Preparation, Characterization, and Gas Permeation Properties," *ACS Symp. Ser.*, **744**, 295 (2000).

Uchytil, P., Petrickovic, R., Thomas, S. and Seidel-Morgenstern, A., "Influence of Capillary Condensation Effects on Mass Transport through Porous Membranes," *Sep. Purif. Tech.*, **33**, 273 (2003).

Uhlhorn, R. J. R., Keizer, K. and Burggraaf, A. J., "Gas Transport and Separation with Ceramic Membranes. Part I. Multilayer Diffusion and Capillary Condensation," *J. Membr. Sci.*, **66**, 259 (1992).

Wang, K., Suda, H. and Haraya, K., "The Characterization of $CO_2$ Permeation in a CMSM Derived from Polyimide," *Sep. Purif. Tech.*, **31**, 61 (2003).

White, L. S., Blinka, T. A., Kloczewski, H. A. and Wang, I., "Properties of a Polyimide Gas Separation Membrane in Natural Gas Streams," *J. Membr. Sci.*, **103**, 73 (1995).

Yoshioka, T., Tanaka, J., Furutani, S., Tsuru, T. and Asaeda, M., "Transport Properties of Condensable Gases through Microporous Silica Membranes," *Trans. Mat. Res. Soc. Japan*, **29**, 3247 (2004).